

Optimization of Frequency Selective Surfaces with Crossed Dipoles Using the Taguchi's Method

Eliel P. Santos, Jannayna D. B. Filgueira, Antonio Luiz P. S. Campos,
Federal University of Rio Grande do Norte, Natal, RN, Brazil e-mails: antonio.luiz@pq.cnpq.br;
elielpoggi@gmail.com; jannadb@gmail.com

Alfredo Gomes Neto

Federal Institute of Paraíba, João Pessoa, PB, Brazil e-mails: alfredogomesjpa@gmail.com

Robson Hebraico C. Maniçoba

State University of Southwest Bahia (UESB), Jequié, Bahia, Brazil, e-mail: robsonhcm@gmail.com

Abstract— There are several techniques for optimization of Frequency Selective Surfaces (FSS). Generally, in literature, we can find a few articles about the Taguchi's method applied in electromagnetic. This method is based on orthogonal arrays (OAs) and it is a procedure that reduces the number of iterations required in an optimization process. For a FSS optimization using the crossed dipole geometry, the Taguchi's method, in combination of the equivalent circuit method, is used for the first time. Here, we applied the method for synthesis of FSS with crossed dipole geometry. The results show that the parameters, of the synthesized FSS, are extracted in an easy and successful way. A prototype was built for validation purpose.

Index Terms— FSS, Taguchi's Method, Equivalent Circuit Method, Optimization.

I. INTRODUCTION

Applications involving Frequency Selective Surfaces require structural projects that works efficiently, leading to a low manufacturing cost and ease of implementation. Because of their frequency selective behavior, these structures have been applied in the areas of microwave and communication systems. The design of these structures involves the study of physical parameters in order to obtain desired operating characteristics.

In this context, optimization techniques can be used in synthesis of frequency selective surfaces to get a good result without compromising performance, while reducing time and cost to design. Some of these techniques are particle swarm optimization (PSO) [1] – [3], artificial neural networks (ANN) [4], [5], genetic algorithms (GA) [6], [7], Multi-objective Optimization [8], etc. Those methods can be divided into two groups: global and local techniques [9]. For applications in electromagnetism, global techniques have some advantages over local techniques, showing better results.

Optimization is a process with the objective to minimize the effort required and maximize the desired result. The optimization methods aim at finding the best results by adjusting the input parameters to improve the performance of a device or system. Nowadays, optimization methods have received attention in various areas of research, including in electromagnetics in which the applications

are diverse and the results are quite satisfactory. Features such as robustness and design flexibility contribute to these techniques what are widely used.

This research has proposed applying, for the first time, the Taguchi method to optimize parameters of the FSS with crossed dipoles, so that the analyzed structures meet a desired frequency response. As analysis method, the improved method of the equivalent circuit [10] was chosen. The equivalent circuit of the crossed dipole is unprecedented. Numerical simulations were performed and a prototype was built and measured. The experimental and numerical results were compared in order to prove the effectiveness of the method.

II. CROSS DIPOLE MODELING USING THE EQUIVALENT CIRCUIT METHOD

The development of equivalent circuits for FSS structures starts with the representation of an infinite array of parallel conductive strips, developed by Marcuvitz [11]. He made the mathematical development of the circuit parameters, however, the first to apply the concept in FSS was Anderson [12] and subsequently Langley and Parker [13], [14] and Lee and Langley [15] developed the method.

According to Marcuvitz the presence of a discontinuity in the structure, results in discontinuity in the fields of the propagating modes at the terminals of a given structure. Discontinuities of a voltage-current or field may be represented by a set of equivalent circuits [11].

The theoretical determination of the parameters of the equivalent circuits require mathematical methods, which are within the microwave-engineering field. Generally, boundary conditions involve solutions or field problems. After the mathematical development on the boundary conditions, the parameters of an infinite array of parallel conducting strips are found.

A periodic array using crossed dipoles is shown in Fig. 1. The periodic array of the crossed dipole has periodicity, p , dipole length, d , strip width, w , and spacing between two dipole arms, g .

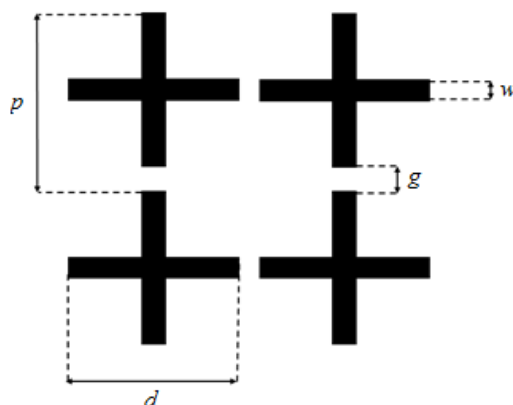


Fig. 1. Periodic array of crossed dipoles.

The shape of the crossed dipole allows separates into perpendicular and parallel conducting strips to the electric field. Parallel strips to the electric field are equivalent to an inductive element and the perpendicular strips to the electric field correspond to a capacitive element. Breaking apart the structure of the crossed dipole in vertical and horizontal strips, we obtain the configuration shown in Fig. 2.

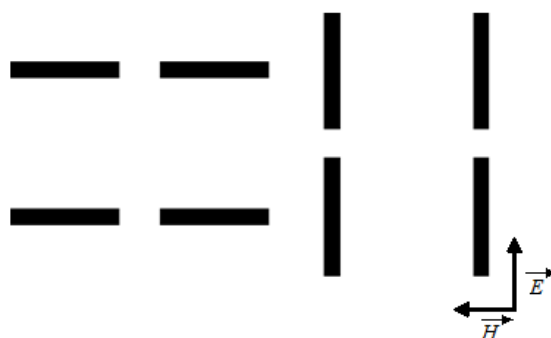


Fig. 2. Crossed dipoles conductive strips separated.

Initially it was used for modeling the crossed dipole FSS a simple LC serial circuit as in array of square loops [13], because of the similarity of how the strips can be separated. However, we observed that the curves of the transmitted power and the reflected power were symmetric and it does not match to the same measurement curves in accordance with the bandwidth and the resonance frequency.

In this article, the proposed equivalent circuit includes the influence of a capacitor in parallel to the LC branch, as shown in Fig. 3. An important observation is not modify the main branch LC (L_1C_1) because it is responsible for the resonant frequency and the configuration reject-band. Then, no element should be put in series or in parallel with C_1 or L_1 . The capacitor C_2 is in parallel with the branch $L_1 - C_1$. In this configuration, the capacitor C_2 does not influence the resonant frequency, but will contribute with the bandwidth.

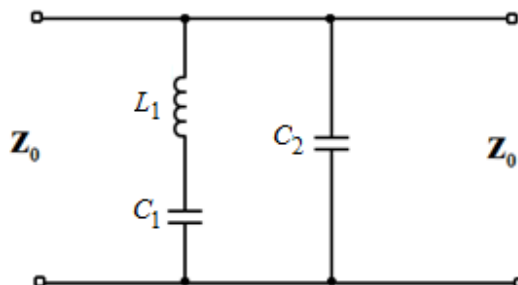


Fig. 3. Proposed equivalent circuit for a FSS with crossed dipoles.

The equivalent circuit for the proposed structure of the crossed dipole is based on the inductive reactance of width w , a capacitive susceptance derived from the spacing $p - w$ and other susceptance derived from the spacing g . According to [11] the inductive reactance and the capacitive susceptance are reduced by a factor d/p due to the strips not be continuous. We noted that for a crossed dipole a finite conducting strip parallel to the electric field is not equivalent to an inductor, but in [16], was demonstrated by Munk that for non-continuous periodic structures, these finite strips must be an associated capacitor. This alternative was used because of the observation that when the frequency is increased, the resonance frequency increased, and this effect was the opposite of what is observed in [16]. The Munk theory meets the need of the use of the factor d/p .

The equivalent circuit was implemented in Matlab and their coefficients were weighted empirically by the method of trying and error. These values were scaled to obtain a coherent bandwidth and

resonant frequency.

The value of the inductive reactance of L_1 is calculated as:

$$\frac{X_{L1}}{Z_0} = 1.3F(p, w, \lambda, \phi) \quad (1)$$

The capacitive susceptance of C_1 is calculated as:

$$\frac{B_{C1}}{Z_0} = 0.17\varepsilon_{eff}B_{Cg} \quad (2)$$

The capacitive susceptance of C_2 is responsible for the asymmetric configuration of the transmission and reception curves. This susceptance is formed by the sum of two other susceptances (B_{Cp-w} and B_{Cg}) and is calculated as:

$$\frac{B_{C2}}{Z_0} = 0.12\varepsilon_{eff}(B_{Cg} + B_{Cp-w}) \quad (3)$$

where,

$$B_{Cg} = 4F(p, g, \lambda, \theta) \quad (4)$$

$$B_{Cp-w} = 4F(p, p - w, \lambda, \theta) \quad (5)$$

θ and ϕ are the incident angles of the plane wave and $F(\cdot)$ is a factor defined in [11 – 15].

The effective permittivity is:

$$\varepsilon_{eff} = \varepsilon_r + (\varepsilon_r - 1) \left(\frac{-1}{e^{Nx}} \right) \quad (6)$$

where $x = 10h/p$, N is an exponential factor, which takes into account the slope of the curve. This parameter varies with the geometry of the element used in the unit cell of the FSS, as a function of the fill factor of the unit cell (metal part in the cell) and h is the thickness of the dielectric.

This circuit has an equivalent admittance equal to:

$$Y = \frac{1}{X_L - \frac{1}{B_{C1}}} - \frac{1}{\frac{1}{B_{C2}}} \quad (7)$$

Finally, the transmission and reflection coefficients are calculated as:

$$\tau = \frac{4}{4 + Y^2} \quad (8)$$

$$\Gamma = \sqrt{1 - \tau^2} \quad (9)$$

III. VALIDATION OF THE EQUIVALENT CIRCUIT MODEL

For validation of the proposed equivalent circuit, we used measurements obtained in [17] and [18] to compare with simulations obtained from the equivalent circuit for the cross dipole array.

Fig. 4 shows a comparison between the numerical results obtained with the equivalent circuit model and measured results obtained in [17]. The dimensions of the structure are: $w = 0.383$ cm, $d = 2.058$ cm, $p = 2.857$ cm, $g = 0.799$, $\varepsilon_r = 4.4$, and $h = 1.6$ mm. To this structure was used an $N = 1.15$. The

structure has a resonance at 5.35 GHz to the results obtained with the equivalent circuit model. The results of the measurements show that the resonance at 5.37 GHz, featuring -0.37% error with respect to resonance frequency. For the bandwidth (BW), the structure had a 680 MHz of BW for the results obtained with the equivalent circuit model. The measurement results show that BW is 700 MHz, featuring -2.86% error.

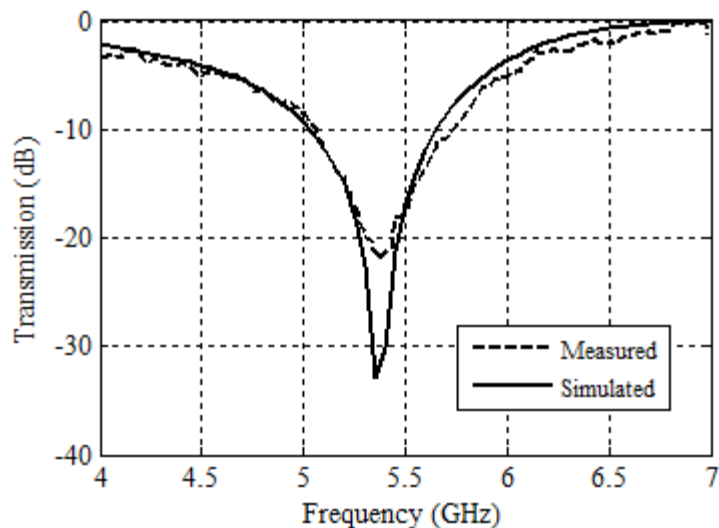


Fig. 4. Comparison between equivalent circuit method and measured results obtained in [17].

Fig. 5 illustrates a comparison between the numerical results obtained with the equivalent circuit model and the measured results obtained in [18]. The dimensions of the structure were $w = 0.12$ cm, $d = 1.2$ cm, $p = 1.5$ cm, $h = 1.6$ mm, $\epsilon_r = 4.4$ and $N = 0.9$. The structure has a resonance that occurs at 8.10 GHz to the results obtained with the equivalent circuit model. The results of the measurements show that the resonance occurs at 8.07 GHz, featuring -0.37% error with respect to resonance frequency. For the bandwidth, the structure had a 725 MHz of BW for the results obtained with the equivalent circuit model. The measurement results show that BW is 750 MHz, featuring 3.33% error.

Fig. 6 illustrates a comparison between the numerical results obtained with the equivalent circuit model and measured results obtained in [18]. The dimensions of the structure were: $w = 0.12$ cm, $d = 1.2$ cm, $p = 2.0$ cm, $h = 1.6$ mm, $\epsilon_r = 4.4$ and $N = 0.57$. The structure has a resonance that occurs at 7.80 GHz to the results obtained with the equivalent circuit model. The results of the measurements show that the resonance occurs at 7.75 GHz, featuring -0.65% error with respect to resonance frequency. For the bandwidth, the structure had a 500 MHz of BW for the results obtained with the equivalent circuit model. The measurement results show that BW is 460 MHz, featuring -8.7% error.

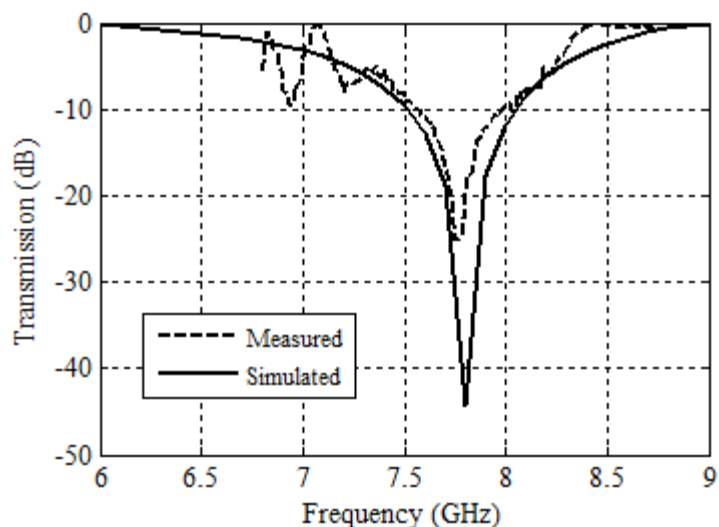


Fig. 5. Comparison between equivalent circuit method and measured results obtained in [18] for $p = 1.5$ cm.

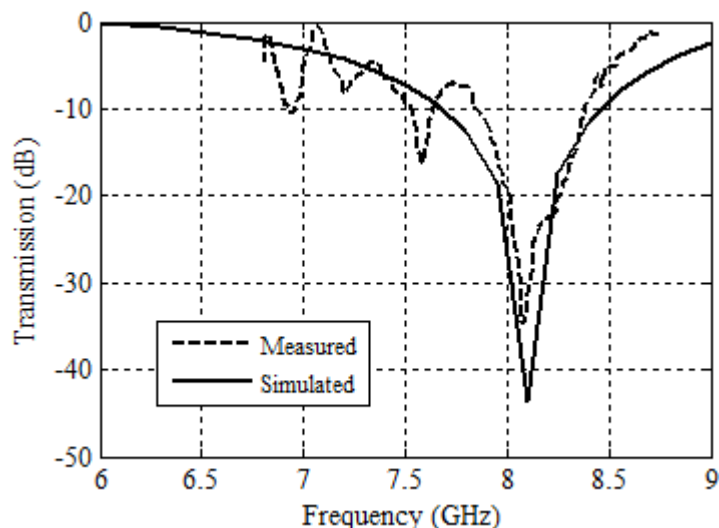


Fig. 6. Comparison between equivalent circuit method and measured results obtained in [18] for $p = 2.0$ cm.

IV. ORTHOGONAL ARRAYS

The Taguchi's method is based on orthogonal arrays (OA) that provide a good way to determine the optimized parameters. These parameters can be optimized with small number of experiments. The notation $OA(N, K, s, t)$ is used to represent an orthogonal array in the Taguchi's method. The variable N is the number of rows in the array, K is the number of columns and s is the number of levels. The variable t is the strength. The K rows of an orthogonal array represent the parameters that need to be optimized and the N lines represent the amount of experiments will be conducted at each iteration of the method [9].

An OA is a matrix A with N rows, K columns and with s entries, that have s levels and strength t ($0 \leq t \leq K$). The lines of the OA is a combination of levels of the parameters that should be optimized. There are a balanced and fair selection of the parameters in all possible combinations. The OA has three properties that are fundamental for the implementation of Taguchi's method. First is the fractional factorial experiments, where the amount necessary to achieve the desired result is reduced.

Second property determines that all possible combinations of parameters occurs equally, which ensures a balanced and fair combination of levels, so all levels of a parameter are tested equally. Third property determines if one or more columns are deleted from an OA, the resulting matrix continues being an OA [9].

In this study, the crossed dipole geometry is considered as unit cell of the FSS. This geometry has three parameters that should be optimized: the periodicity p , the length of the dipole d , and the width of the strip w , as can be seen in Fig. 1. So, based on that information, the OA used is shown in Table I.

TABLE I. TYPE SIZES AND APPEARANCE

Experiment	Parameters		
	p	d	w
1	1	1	1
2	1	2	3
3	1	3	2
4	2	2	2
5	2	3	1
6	2	1	3
7	3	3	3
8	3	1	2
9	3	2	1

V. TAGUCHI'S METHOD

The optimization process begins with the selection of a suitable Orthogonal Array and the fitness function or adaptive function. The selection of an OA depends mainly on the number of parameters being optimized. Fig. 7 illustrates the flowchart for implementing the Taguchi's method [9].

At the first iteration the Level 2 is selected in the centre of optimizing range, as:

$$N_2 = \frac{\min + \max}{2} \quad (10)$$

where \min and \max correspond to the lower and upper limits of optimization interval. Levels 1 and 3 are obtained by subtracting and adding, respectively, the value of Level 2 with a variable level difference (LD), as:

$$N_1 = N_2 - LD_i \quad (11)$$

$$N_3 = N_2 + LD_i \quad (12)$$

The level difference of the first iteration is determined by [9]:

$$LD_1 = \frac{\max - \min}{\text{level number} + 1} \quad (13)$$

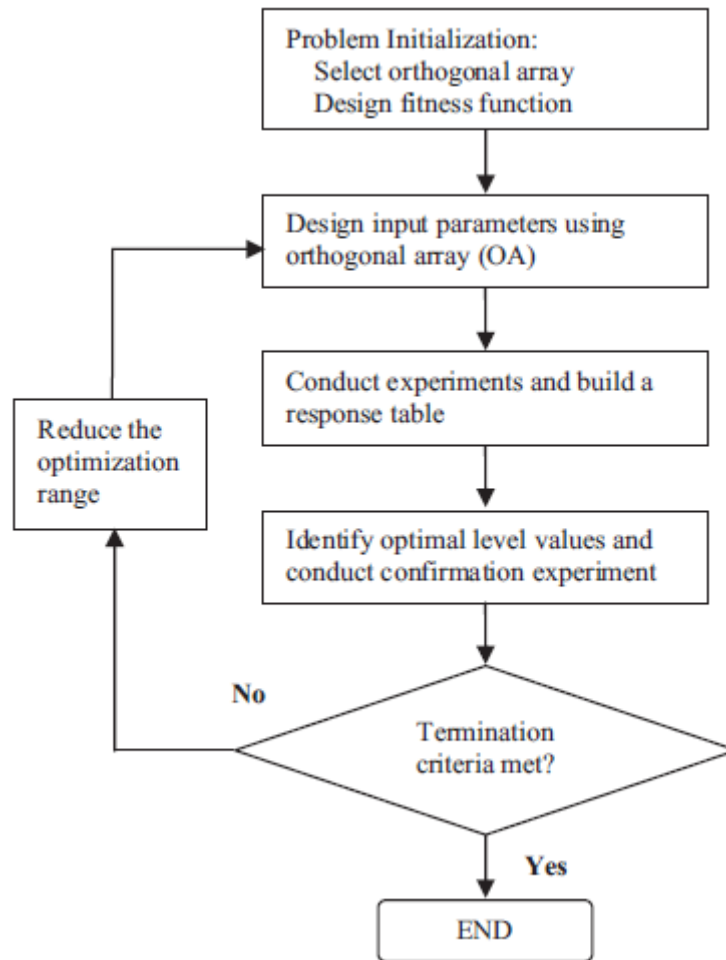


Fig. 7. Flowchart of the Taguchi's Method.

After determination of the input parameters' levels, the fitness function for each experiment can be calculated. So, the fitness function value is converted to signal to noise ratio (η) as [9]:

$$\eta = -20 \log(\text{FF}) \text{ dB} \quad (14)$$

where FF is the fitness function.

The fitness function results are used to construct a response table for each iteration through signal to noise ratio average, for each parameter and level using:

$$\bar{\eta}_{m,n} = \frac{S}{N} \sum_{i, OA(i,n)=m} \eta_i \quad (15)$$

The best level for each parameter is obtained from the response table. For each iteration the optimization interval is reduced until a convergence value. For this purpose, LD_i is multiplied by a rate (rr) to obtain the level difference for the next iteration ($i + 1$):

$$LD_{i+1} = rr \cdot LD_i = rr^i \cdot LD_1 = RR(i) \cdot LD_1 \quad (16)$$

where $RR(i)$ is the reduction function. The value of rr may be adjusted between 0.5 and 1.0 depending on application. When a constant rr is used $RR(i) = rr^i$. For bigger values of RR , the rate of convergence is more slower.

The finish criteria for the optimization process is:

$$\frac{LD_i}{LD_1} < \text{convergence value} \quad (17)$$

The convergence value can be between 0.001 and 0.01. The optimization process is finished when an adopted condition is satisfied [19] - [22].

In some applications the solution of the optimization process are located near the optimization interval ends. In this case, to improve the performance of the Taguchi's Method the initial level difference (LD_1) is increased by 1.5 times, so that the optimization process has a greater range to find the best result.

We also need to treat the limits, because the optimization process may provide values out of the range established. In this case, when the level 2 of an iteration reaches the minimum value of the optimization range, the next iteration will have their values of level 1, level 2 and level 3 recalculated as:

$$N_1 = \text{min} \quad (18)$$

$$N_2 = \text{min} + LD_{i+1} \quad (19)$$

$$N_3 = \text{min} + 2LD_{i+1} \quad (20)$$

where *min* is the minimum value of the optimization range.

On the other hand, if the value of level 2 reaches the maximum value of the optimization range, the levels will be recalculated as:

$$N_3 = \text{max} \quad (21)$$

$$N_2 = \text{max} - LD_{i+1} \quad (22)$$

$$N_1 = \text{max} - 2LD_{i+1} \quad (23)$$

where *max* is the maximum value of the optimization range.

In this article we looked at the need to apply the treatment of limits adjustment to achieve satisfactory results.

VI. OPTIMIZATION

For the optimization purpose, the geometry of the FSS structure considered was the crossed dipole. The parameters to be optimized are determined according to each FSS. In this geometry, the optimized parameters are the periodicity, p , the length of the loop, d , and the width of the strip, w .

The optimization process begins with the determination of OA and FF. The OA used was OA (9,3,3,2), because it is the appropriated OA for the crossed dipole. The FF is chosen according to the purpose of optimization. The FF used is:

$$FF = 2 * |f_{ci} - f_{ci}'| + |f_r - f_r'| + 2 * |f_{cf} - f_{cf}'| \quad (24)$$

where f_{ci} and f_{cf} are the lower and higher cutoff frequencies desired, respectively, and f_{ci}' and f_{cf}' are the lower and higher cutoff frequencies obtained, respectively. f_r and f_r' are the resonant frequencies

desired and obtained, respectively. We put a higher weight for the bandwidth than to resonant frequency.

The characterization of the FSS begins with the required parameters such as the bandwidth and resonant frequency. Once established the required parameters, a parametric analysis was performed using data obtained by Equivalent Circuit Method.

For all the parameters to be optimized, we define the optimization range within which the Taguchi's method will run and set the best value for each parameter. This range is consistent with our manufacturing limitations and are presented in Table 2:

TABLE II. OPTIMIZATION PARAMETERS RANGE

Parameter	Optimization Range (cm)
P	1.0 – 2.2
D	0.8 – 2.0
W	0.05 – 0.50

Set optimization intervals and structure parameters, starts the optimization process by Taguchi's method. It is known that in first iteration, level 2 of each parameter is selected in the centre of the optimization range and levels 1 and 3 are calculated by adding and subtracting the value of level 2 with LD .

For example, calculating levels and LD for the parameter p we obtain:

$$N_{2,p} = \frac{\min + \max}{2} = \frac{1.0 + 2.2}{2} = 1.6 \text{ cm}$$

$$LD_{1,p} = \frac{\max - \min}{\text{level number} + 1} = \frac{2.2 - 1.0}{3 + 1} = 0.3 \text{ cm}$$

$$N_{1,p} = N_{2,p} - LD_{1,p} = 1.6 - 0.3 = 1.3 \text{ cm}$$

$$N_{3,p} = N_{2,p} + LD_{1,p} = 1.6 + 0.3 = 1.9 \text{ cm}$$

This is made for the other parameters d and w . Given the initial values of the parameters, the FF for each experiment can be obtained.

For each combination given in Table I, the equivalent circuit method is executed, the fitness function is calculated, and from (14), fitness values are converted to SNR.

After this, (15) is used to obtain a response table that group the SNR mean for the levels of each - parameter. After the first iteration we obtain the response table listed at Table III.

In according with Table III, the best SNR for each parameter is: level 3 for p , level 2 for d , and level 1 for w . The highest S/N for each parameter of Table III corresponds to the optimal level for this parameter. These levels are considered as the level 2 values of the next iteration, so that the other levels (1 and 3) will be reset and recalculated.

The proposed FSS should have the frequency behavior that shows a bandwidth of 1 GHz (7.0 - 8.0

GHz) and a resonance frequency of 7.48 GHz (geometric mean of 7.0 and 8.0 GHz). The optimization for the crossed dipole FSS met the termination criteria after 17 iterations of the method. We used a stop criteria of $rr = 0.75$ and a convergence value of 0.01. Fig. 8 illustrates the convergence curve for the periodicity, p . As we can see, at 17 iterations we obtain a convergence.

TABLE III. RESPONSE TABLE FOR THE FIRST ITERATION

Level	SNR Parameter		
	P	d	w
1	-25.5813	-22.2425	-15.3673
2	-20.5443	-10.7528	-19.1523
3	-10.1531	-23.3104	-21.7591

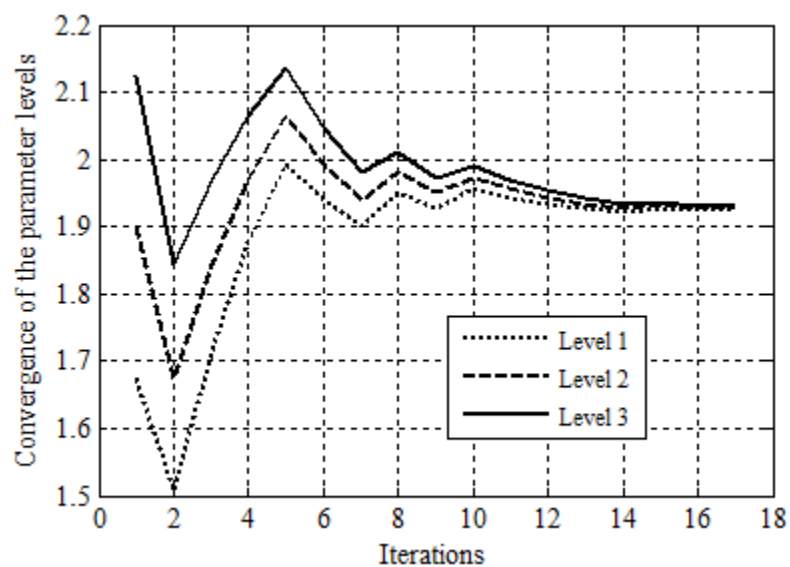


Fig. 8. Convergence of the parameter levels for periodicity.

Fig. 9 and 10 illustrates the convergence for d and w parameters.

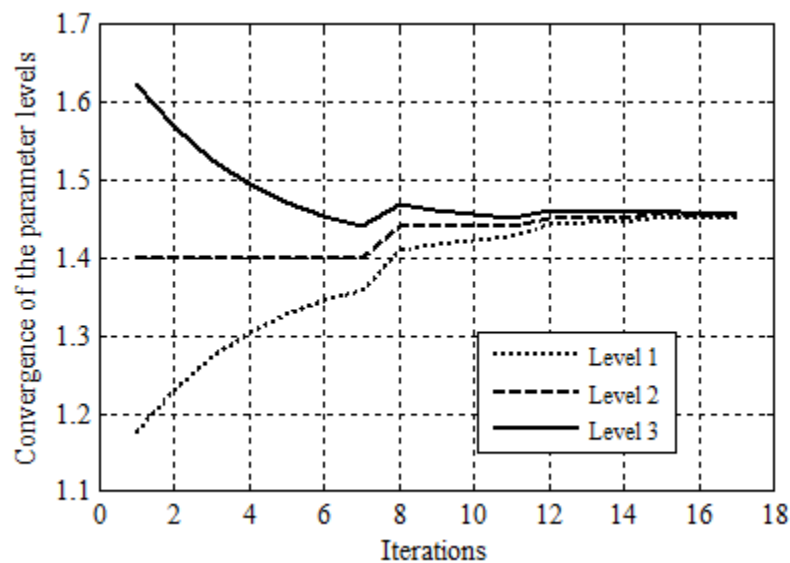


Fig. 9. Convergence of the parameter levels for dipole length.

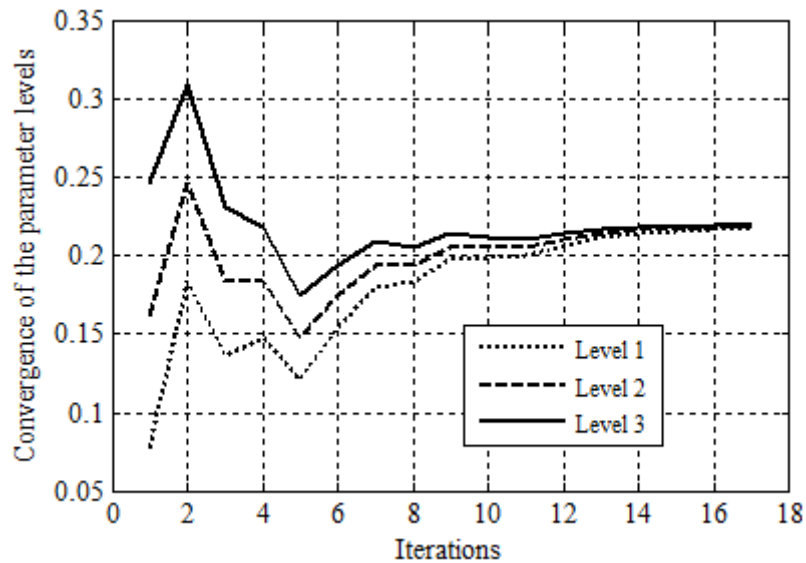


Fig. 10. Convergence of the parameter levels for strip width.

So, optimizing the FSS parameters using a combination of the Taguchi's method with the equivalent circuit method, we obtained $p = 19.261$ mm, $d = 14.571$ mm, and $w = 2.196$ mm. Because of our manufacturing limitations, we choose the values: $p = 19.3$ mm, $d = 14.6$ mm, and $w = 2.2$ mm. The dielectric layer was the FR-4 ($\epsilon_r = 4.4$ and $h = 1.6$ mm). After that, the FSS was built and measurement results were obtained using a Network Analyzer E5071C, for validation of the optimization technique. Fig. 11 illustrates the measurement setup and Fig. 12 illustrates the built FSS.

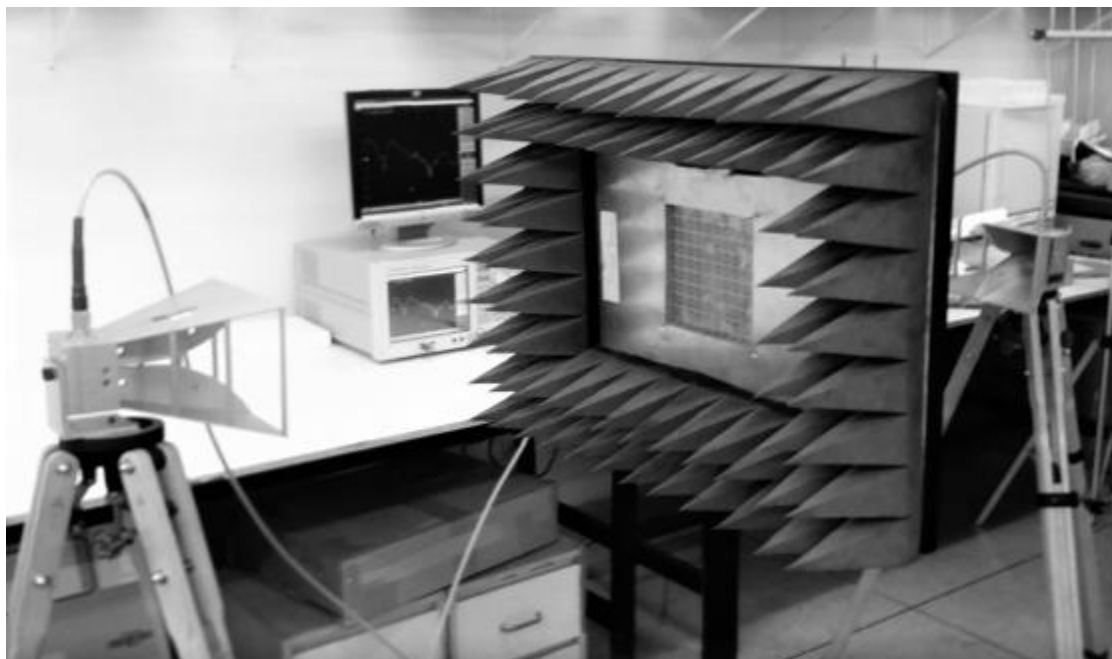


Fig. 11. Measurement setup.

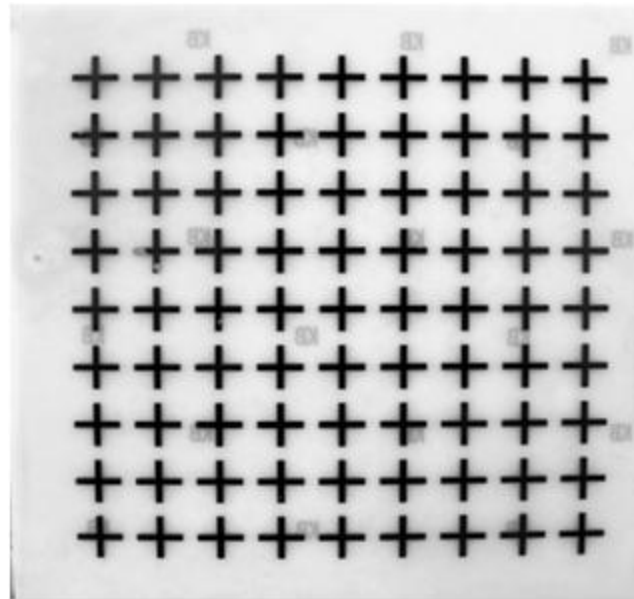


Fig. 12. Built optimized FSS.

Numerical and experimental results were compared as illustrated in Fig. 13. We can observe a good agreement between the results. The bandwidth measured was 0.95 GHz while the desired was 1.00 GHz, an error of 5 %. The resonance frequency measured was 7.50 GHz and the desired was 7.48 GHz, an error of 0.26 %. Differences between simulated and measured results occurs because of the manufacturing process or the measurement environment.

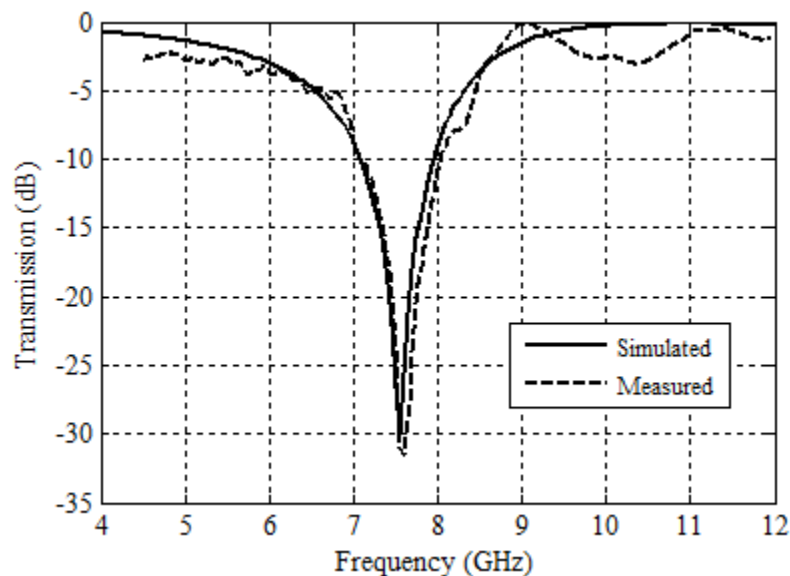


Fig. 13. Comparison between simulated and measured results.

VII. CONCLUSIONS

In this article, we present a new hybrid technique to optimize frequency selective surface parameters. This technique uses a combination of the Taguchi's method with the equivalent circuit method. The treatment of the limits was detailed. One geometry was considered in the analysis, the crossed dipole. A very fast convergence was observed in optimization. We have built and measured a

prototype to validate the proposed technique. We have obtained a good agreement between simulation and measurement results. The proposed technique was applied for the first time on crossed dipoles FSS optimization.

ACKNOWLEDGMENT

The authors express their sincere thanks to National Council of Research and Development – CNPq for supporting the research work over the project 303693/2014-2.

REFERENCES

- [1] Gies, D. and Rahmat-Samii, Y., 'Particle Swarm Optimization for Reconfigurable Phased Differentiated Array Design', *Microwave and Optical Technology Letter*, 2003, **38**, (3), pp 168–175.
- [2] Samsuzzaman, M., Islam, M. T., Kibria, S., and Cho, M., 'A Compact Circularly Polarized High Gain S-band Nano Satellite Antenna Using Ramped Convergence Particle Swarm Optimization'. *Microwave and Optical Technology Letters*, 2015, **57**,(6), pp 1503–1508.
- [3] Yilmaz, A. E. and Kuzuoglu, M., 'Design of the Square Loop Frequency Selective Surfaces with Particle Swarm Optimization via the Equivalent Circuit Model', *Radioengineering*, 2009, **18**, (2), pp 95-102.
- [4] Alcantara Neto, M. C., *et al.*, 'Bioinspired Multiobjective Synthesis of X-band FSS via General Regression Neural Network and Cuckoo Search Algorithm'. *Microwave and Optical Technology Letters*, 2015, **57**, (10), pp 2400–2405.
- [5] Silva, P. H. da F., Cruz, R. M. S. and d'Assunção, A. G., 'Blending PSO and ANN for Optimal Design of FSS Filters with Koch Island Patch Elements', *IEEE Transactions on Magnetics*, 2010, **46**, (8), pp 1-4.
- [6] Campos, A. L. P. S., Martins, A. M. and Almeida Filho, V. A., 'Synthesis of Frequency Selective Surfaces Using Genetic Algorithm Combined with The Equivalent Circuit Method'. *Microwave and Optical Technology Letters*, 2012, **54**, (8), pp 1893–1897.
- [7] Singh, D., Kumar, A., Meena, S., and Agarwala, V., 'Analysis of Frequency Selective Surfaces for Radar Absorbing Materials', *Progress In Electromagnetics Research B*, 2012, **38**, pp 297-314.
- [8] Kuwahara, Y., 'Multi-objective Optimization Design of Yagi-Uda Antenna', *IEEE Transactions on Antennas and Propagation*, 2005, **53**, (6), pp 1984–1992.
- [9] Weng, W. C., Yang, F., and Elsherbeni, A., 'Electromagnetics and Antenna Optimization Using Taguchi's Method' (Morgan & Claypool Publishers 2007).
- [10] Araujo, G. L. R., Campos, A. L. P. S; Martins, A. M., 'Improvement of the Equivalent Circuit Method for Analysis of Frequency Selective Surfaces Using Genetic Algorithms and Rational Algebraic Models'. *Progress in Electromagnetics Research Letters*, 2015, **55**, pp 67-74.
- [11] Marcuvitz, N., 'Wave guide Handbook' (McGraw-Hill 1951).
- [12] Anderson, I., 'On the theory of self-resonant grids', *Bell Syst. Tech. J.*, 1975, **54**, (10), pp 1725–1731.
- [13] Langley, R. J. and Parker, E. A., 'Equivalent circuit model for arrays of square loops', *Electronics Letters*, 1982, **18**, (7), pp 294-296.
- [14] Langley, R. J. and Parker, E. A., 'Double-square frequency selective surfaces and their equivalent circuit', *Electronic Letters*, 1983, **19**, (17), pp 675 - 677.
- [15] Lee, C. K. and Langley, R. J., 'Equivalent circuit models for frequency selective surfaces at oblique angles of incidence', *IEE Proceedings*, 1985, **132**, (6), pp 395 – 399.
- [16] Munk, B. A., 'Frequency Selective Surfaces – Theory and Design' (John Wiley and Sons, Inc. 2000).
- [17] Kiani, G. I., Weily, A. R., and Esselle, K. P. 'A Novel Absorb/Transmit FSS for Secure Indoor Wireless Networks With Reduced Multipath Fading', *IEEE Microwave and Wireless Components Letters*, 2006, **16**, (6), pp 378-380.
- [18] Cruz, R. M., 'Analysis and Optimization of Frequency Selective Surface Using Neural Networks and Artificial Natural Optimization Algorithms (in portuguese)'. Universidade do Rio Grande do Norte, Natal. 2005.
- [19] Pelosi, G., Selleri, S. and Taddei, R., 'A Novel Multiobjective Taguchi's Optimization Technique for Multibeam Array Synthesis'. *Microwave and Optical Technology Letters*, 2013, **55**, (8), pp 1836–1840.
- [20] Li, X., Wang, Z. and Fang, S., 'An Accurate Effective Radius Formula Based on Taguchi Method for Calculating Resonant Frequency of Electrically Thin and Thick Circular Patch Antennas'. *Microwave and Optical Technology Letters*, 2015, **57**, (11), pp 2567–2572.
- [21] Sarshenasandand, M. and Firouzeh, Z. H., 'A Robust Hybrid Taguchi-Gradient Optimization Method for the Calculation of Analytical Green's Functions of Microstrip Structures', *IEEE Antennas and Wireless Propagation Letters*, 2015, **14**, pp 1366-1368.
- [22] Filgueira, J. D. B., Campos, A. L. P. S., Gomes Neto, A., and Maniçoba, R. H. C., 'Calculation of optimized parameters for the frequency selective surfaces by means of Taguchi's method'. *Microwave and Optical Technology Letters*, 2016, **58**, (8), pp 1984–1989.